RESEARCH ARTICLE | FEBRUARY 11 2021

Mechanisms of low-frequency dielectric barrier discharge (DBD) plasma driven by unipolar pulses and bipolar pulses

Hoa Thi Truong ; Yoshihiko Uesugi; Xuan Bao Nguyen

AIP Advances 11, 025022 (2021)
https://doi.org/10.1063/5.0033846

Mechanisms of low-frequency dielectric barrier discharge (DBD) plasma driven by unipolar pulses and bipolar pulses

Cite as: AIP Advances 11, 025022 (2021); doi: 10.1063/5.0033846
Submitted: 23 October 2020 • Accepted: 12 January 2021 •
Published Online: 11 February 2021

Hoa Thi Truong,[1,a] Yoshihiko Uesugi,[2,b] and Xuan Bao Nguyen[1]

AFFILIATIONS

[1]The University of Danang, University of Technology and Education, Da Nang City, Vietnam
[2]Emeritus, Nagoya, Aichi Prefecture 461-0023, Japan

[a]**Author to whom correspondence should be addressed:** tthoa@ute.udn.vn and hoa03d4@gmail.com
[b]**Email:** uesugi1@mac.com

ABSTRACT

In this study, experimental results presenting the development of Dielectric Barrier Discharge (DBD) powered by bipolar and unipolar pulses are compared. The experimental results showed that discharge current peaks in the case of DBD driven by repetitive unipolar pulses were about three times lower than those in the case of DBD driven by bipolar pulses. It is well known that if DBD is driven by bipolar pulses, the effect of surface charge on dielectric layers from the preceding discharge helps to ignite consecutive discharges at the same locations where the previous discharges already struck. In contrast, in the case of DBD generated by using the low-frequency unipolar pulses, the consecutive DBDs just could be initiated after the system erases part of the prehistory effect of surface charge deposition on dielectric layers from the preceding discharge, and then the following discharge was ignited at erased or uncharged areas. It was critical that a part of the energy stored in the dielectric layer and discharge gap by the previous discharge needed to be released to develop the next discharge. The results of this study provided an outlook for estimating the effectiveness of the DBD plasma system used in specific applications such as DBD for flow actuators or surface treatment where the use of unipolar DBDs at low frequency may be necessary.

I. INTRODUCTION

Dielectric barrier discharge (DBD) plasma has drawn much attention due to the advantage of the existence of free radicals and high energy electrons at low gas temperature and atmospheric pressure.[1–4] From the first application of being used for generating ozone,[1,5] nowadays, the application of DBD plasmas has opened up to various fields such as light sources,[1,4] surface treatment,[1,4] environmental treatments (e.g., toxic gas decomposition),[6] water treatment,[7,8] and medical treatment.[9,10]

The DBD is a discharge type generated in a space gap between electrodes in the presence of one or more dielectric layers. The dielectric is an insulator and cannot transmit direct currents. Therefore, DBDs are well known to be generated by alternating current high voltage sources or high-frequency nano-pulse sources.[1,4] At atmospheric pressure, DBDs are generally operated in filament mode in the form of individual breakdown channels called micro-discharges.[11,12] During discharge, free charged particles will accumulate on the surface of dielectric layers. The accumulation of charges on the dielectric layer induces the effects called "memory effects" and an electric field in discharge space. The induced electric field (E) is in the opposite direction with the external electric field and, hence, prevents the micro-discharge channels from transferring to the arc and characterizes DBD as a self-pulsing discharge.[1–4,11] Because of "memory effects," if DBD is driven by a high-frequency high voltage alternating current power supply, the effects tend to ignite the next discharges in subsequence one-half cycle at the locations where the previous discharges have already struck in the previous half cycle with opposite polarity. On the other hand, for the case of DBD excited by high-frequency repetitive pulse with very short rise time, the "memory effect" from the primary discharge at a rising slope of high voltage pulse will initiate a secondary

discharge at a falling slope of the pulse. It seems that the secondary discharge developed along the conductive channel of the primary discharges.[1,11]

In most cases, the use of high-frequency bipolar pulses or short rising time square unipolar pulses for generating DBD is preferred to the use of low-frequency unipolar pulse with the relative long rise of fall time since the utilization of the electrostatic energy from "memory effect" is possibly a means to improve the efficiency of the DBD system.[13,14] However, these DBD systems are expensive due to the high price of power sources. Furthermore, in many applications such as surface dielectric barrier discharge (SDBD) for flow actuators or electrohydrodynamic (EHD) control and surface treatment, the employment of low-frequency unipolar pulses with a relative long falling time is necessary since it can help to spread the discharge to over the dielectric surface or expand the area occupied by surface charges and reduce the effect of overheating on the treatment surface.[15–19] According to the results found in the work of Benard and Moreau,[20] surface charge and voltage waveform are two of the key parameters for the performance of the surface DBD actuators. A reduction in the charge accumulation at the dielectric surface is a potential method for increasing electrohydrodynamic force. In addition, it is found in the work of Bernard and Moreau,[20] Thomas *et al.*,[21] and Dyken *et al.*[22] that among different kinds of voltage waveforms used for exciting the DBD actuator, a higher thrust is produced at a given consumed power when a negative saw-tooth voltage waveform is used. Although, in the literature, the role of the "memory effects" in characteristics of the DBDs generated by high-frequency high voltage pulses with very short rising and falling time (around tens of nanoseconds) has been extensively investigated.[23–25] Nevertheless, the mechanism and characteristic of low-frequency DBD driven by unipolar high voltage pulses with a long rise or fall time or unipolar high voltage pulses with saw-tooth waveforms and the surface charge diffusion have not been fully explored.

Low-frequency DBD operation exposes different characterization from high-frequency DBD operation, especially in some kinds of DBD reactors such as glass type.[26] Under such low frequency operating conditions, displacement current is separated from the discharge current. Therefore, the discharge current is recorded with high accuracy. In addition, in many applications, DBDs are constrained by complexity and the high price of power supply. So far, to make the DBD plasma more applicable and less expensive, there are many efforts to generate and simplify DBD by less expensive high voltage pulse power supplies.[27–29] In our previous study, silicone diodes for alternating current (SIDAC) have been used to manipulate high voltage pulses.[28] If the connection of a number of SIDACs in series is connected to a DC high voltage power supply, the train of unipolar pulses is generated. Otherwise, if this connection is connected to a primary AC power supply, the bipolar pulses will be manipulated.[26,29]

This study provides a deeper insight into the processes of the discharges sustained by low-frequency unipolar pulses with a long rise or fall time in a reactor with two electrodes covered by dielectrics. The processes are studied by comparing the electrical characteristics of DBDs powered by bipolar and unipolar pulses. Once the unipolar pulses are a quasi-like saw-tooth waveform that excites DBD accompanied with the diffusion of the accumulated surface; charges on the dielectric layer could be beneficial for the application of surface DBD in actuators. This study will provide a starting point for optimizing the discharge properties used in specific applications such as dielectric barrier discharge (DBD) for flow actuators where the use of unipolar DBDs at low frequency may be necessary. The discharges were generated in a glass reactor with low-frequency bipolar and unipolar pulses manipulated using SIDACs.

II. SILICON DIODES FOR ALTERNATING CURRENT (SIDAC)

Silicon Diodes for Alternating Current (SIDAC) works as a switch with the V–I characteristic SIDAC shown in Fig. 1. As shown in Fig. 1, the break-over voltage (V_{BO}) and holding current (I_H) are two thresholds governing the switching operation. If a voltage applied to SIDAC is less than the break-over voltage (V_{BO}), SIDAC is in a non-conducting state (the red line). When the applied voltage is increased to meet or exceed the value of (V_{BO}), the SIDAC will switch to become conductive and enters to the transition region (green line) within an ns transiting time scale. The conducting state (blue line) is sustained until the current through SIDAC is still higher than the holding current (I_H). If the number of SIDACs in the series connection is N, the break-over voltage of this connection will be increased to N times, but the holding current (I_H) is kept the same as single.

The operation of the SIDAC connection is tested by a circuit diagram shown in Fig. 2. In the test experiment, ten SIDACs [Model No. K1V38 (W), V_{BO} ~ 380 V, I_{BO} = 50 mA, Shindengen Electric Mfg. Co., Ltd.] were connected in series. A typical break-over voltage and switching time of the SIDAC connection had also been experimentally examined as 3600 V–4000 V in about 200 ns by Sumiishi *et al.*[29] When the connection of SIDAC is switched to become conductive, a high voltage pulse of up to 4000 V will be generated. The SIDAC connection was experimentally tested with a load of 40 kΩ resistor. The circuit was powered by a direct current (DC) primary power supply with an input voltage of about 6 kV. The experimental result is demonstrated in Fig. 3 with the typical waveforms of voltage on the capacitor (1.25 nF) (v_C), voltage on the SIDAC connection (v_{SIDAC}), voltage on the resistor (v_R), and current through

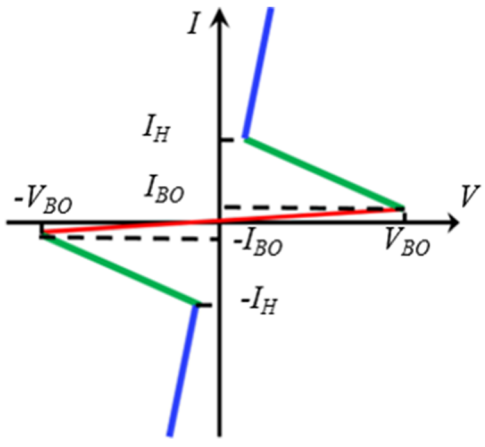

FIG. 1. V–I characteristic of SIDAC.

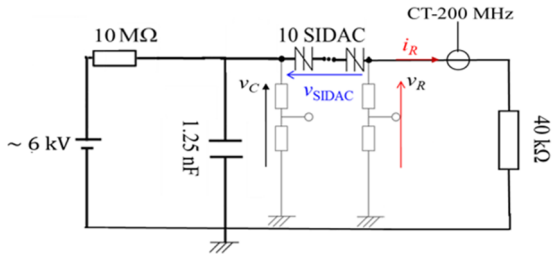

FIG. 2. Circuit test diagram for the operation of SIDAC connection.

load resistor (i_R). While the voltage on the capacitor (v_C) and the voltage on the resistor (v_R) are obtained by high voltage dividers (EP 50K, NPE, 2000:1, DC-50 MHz), the voltage on the connection of SIDACs (v_{SIDAC}) is determined by the difference between the other voltages as follows:

$$v_{SIDAC} = v_C - v_R.$$

As shown in Fig. 3, before switching, SIDACs are in a nonconductive state and disconnect the resistor from the capacitor, the voltage on the capacitor is charged up by the primary DC input power, the voltage on the resistor is nearly equal to zero, and the voltage on the connection of SIDACs (v_{SIDAC}) is nearly equal to the voltage on the capacitor (v_C) [blue curve (v_{SIDAC}) meets black curve (v_C)]. When the voltage (v_C) is charged up to exceed the break-over voltage (V_{BO}) of the SIDAC connection (~4000 V), the SIDACs are switched and rapidly transited to the transition region. Simultaneously, a high voltage pulse is applied to the load of the resistor. During the transition state of SIDACs, the voltage on the capacitor (v_C) is discharged through the load of 40 kΩ, and the current flow through the circuit decreases exponentially. When the current is smaller than the holding current (I_H = 50 mA), the SIDACs are turned to the blocking state. Consequently, the resistor and the capacitor are electrically

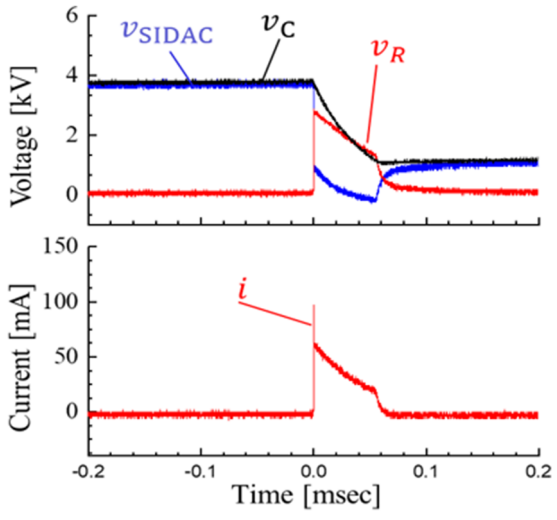

FIG. 3. Results of operation of SIDAC connection.

isolated, the voltage on the resistor and its current drop, the voltage on the capacitor starts being charged up again, the voltage on the SIDAC connection starts increasing again, and one working cycle is completed.

III. EXPERIMENTAL SETUP

The experimental setup used for the generation of DBDs by using SIDACs in the gas phase in a glass reactor has been partially described in our former works,[26,28] so in this paper, only the principle of the experimental setup is presented here. A view of the equipment setup and a schematic of the electric circuit of DBD plasma generation and condition in both cases of DBD generating by using unipolar pulses and bipolar pulses are shown in Fig. 4 and Table I, respectively. In this setup, ten SIDACs [Model No. K1V38 (W), Shindengen Electric Mfg. Co., Ltd.] in series connection were utilized to manipulate the pulses for DBD generation. If the connection is connected serially to a DC high voltage power supply, the train of unipolar pulses is generated. Otherwise, if this connection is connected serially to an AC power supply, the bipolar pulses will be

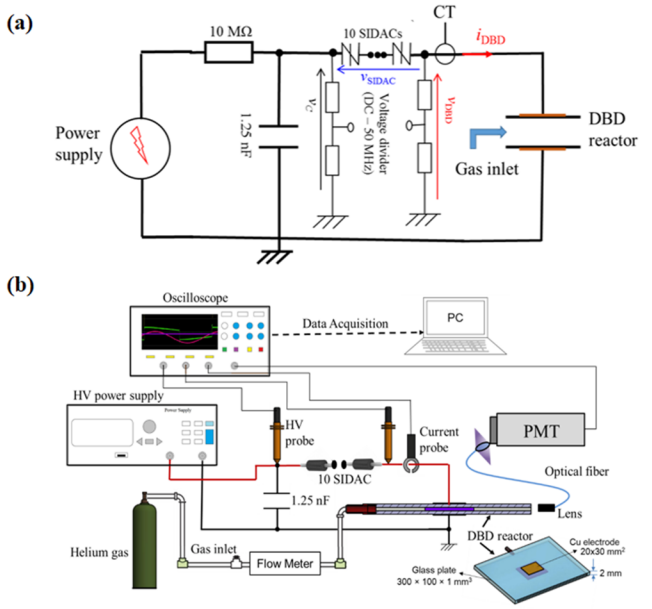

FIG. 4. Experimental setup: (a) circuit diagram and (b) schematic diagram for the DBD system.

TABLE I. Condition of experiment with the AC power supply.

Primary power supply	AC/9 kVpp/60 Hz DC 6.5 kV/−6.5 kV
Working gas	He
Gas flow	500 SCCM
Photomultiplier voltage	800 V
Pressure	Atmospheric pressure
Sample time	500 ps
The number of samples per second	2 GSa/s

manipulated. A capacitor of 1.25 nF was used to stabilize the waveform of the supply voltage. A resistor of 10 MΩ was used to limit the current fed to the capacitor in order to protect the power source.

The planar reactor is glass plates of 300 × 100 × 1 mm^3 in size. The discharge gap is 2 mm. Copper foils of 20 × 30 mm^2 were used as electrodes. Three sides of the reactor were sealed, and one side was opened for a gas outlet. A pipe for the gas inlet was located and inserted on the wall of the gap. Helium working gas was injected into the discharge area through the pipe at a flow rate of 500 SCCM. The optical emission from the discharge volume was detected by using a photomultiplier tube (PMT) (Hamamatsu R928-rise time of 2 ns and transit time of 22 ns) at an applied voltage of 800 V.

Voltages on both sides of the SIDAC connection were measured by a high voltage probe (EP 50K, NPE, 2000:1, DC-50 MHz) with a resistance of 500 M**Ω** that indicates the voltage on the charge capacitor (1.25 nF) and the voltage on the DBD reactor, and the voltage on SIDAC is defined as the difference between voltages on the above two voltages. Currents were monitored by using a current transformer (CT) (Pearson Model 2877-200 MHz) installed at the high voltage side of the reactor. The waveforms were obtained by using a wideband digital Agilent oscilloscope of DSO 6054A (500 MHz) with a sample rate of 2 GSa/s. The unipolar pulses were generated by connecting SIDACs to a DC power supply of around 6.5 kV or −6.5 kV output voltage, and the bipolar pulses were generated by using the AC power supply of 9 kVp-p output voltage at a frequency of 60 Hz.

IV. EXPERIMENTAL RESULTS AND DISCUSSION

The results of the experiments are shown in Figs. 5–8. In these figures, typical waveforms of voltages on the charge capacitor (1.25 nF) (v_C), voltages on the series connection of SIDAC (v_{SIDAC}), voltages on the DBD reactor (v_{DBD}), currents flow through the DBD reactor, powers as products of the voltage (v_{DBD}) multiplied to the current, and intensity of light emitted from the plasma are illustrated.

The experimental results obtained in the case of DBD powered by the unipolar pulses with both positive pulses and negative pulses are shown in Figs. 5 and 6. The experimental results obtained in the case of DBD powered by bipolar pulses are shown in Figs. 7 and 8.

As can be seen from these figures, every time when SIDACs are switched on, simultaneously, a voltage pulse with a sharp change of about 4 kV within nearly 200 ns will be generated and applied to the DBD reactor. As can be observed from the overall waveforms shown in Figs. 5 and 7, following a voltage pulse applied to the reactor, the discharge occurs. The time intervals between discharges are about 20 ms and 10 ms in the case of using a primary DC power supply for both polarities [Figs. 5(a) and 5(b)] and the case of a primary AC power supply (Fig. 7), or unipolar (positive or negative) pulses and bipolar pulses, respectively.

In the case of the DBD driven by unipolar pulses, the primary input voltage imposed on one side of the SIDAC connection (v_C)

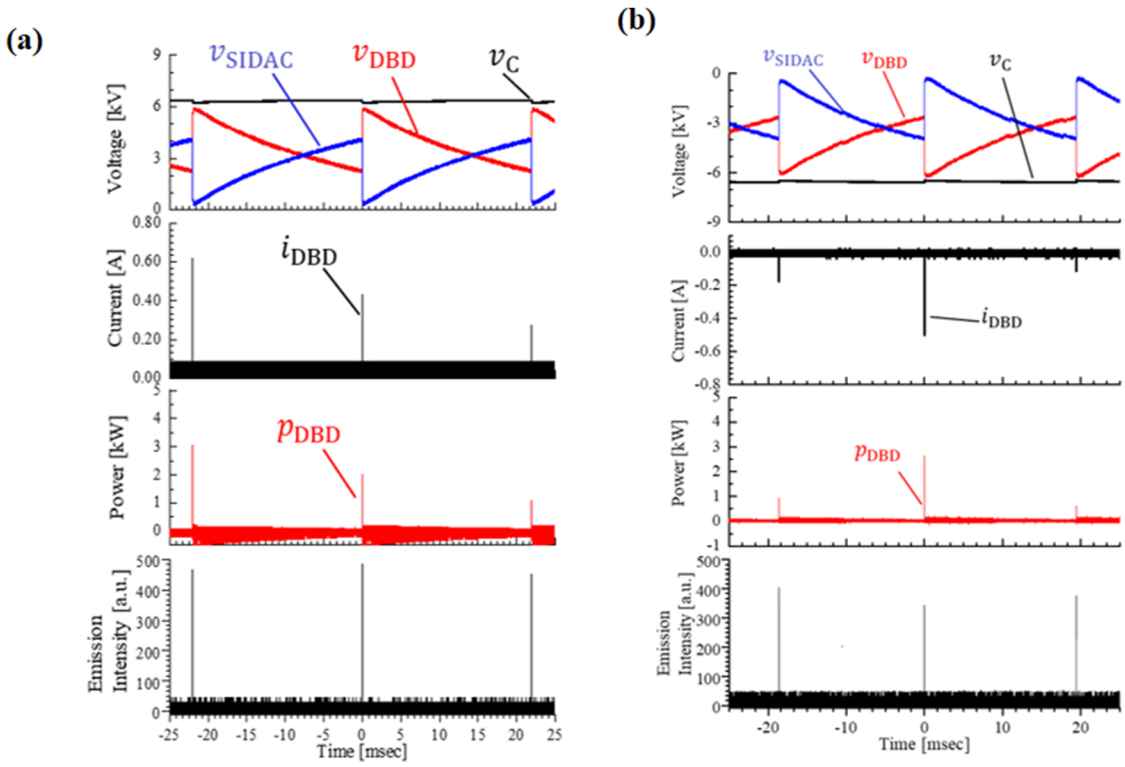

FIG. 5. Overall waveforms of DBDs generated by unipolar pulses: (a) positive case and (b) negative case.

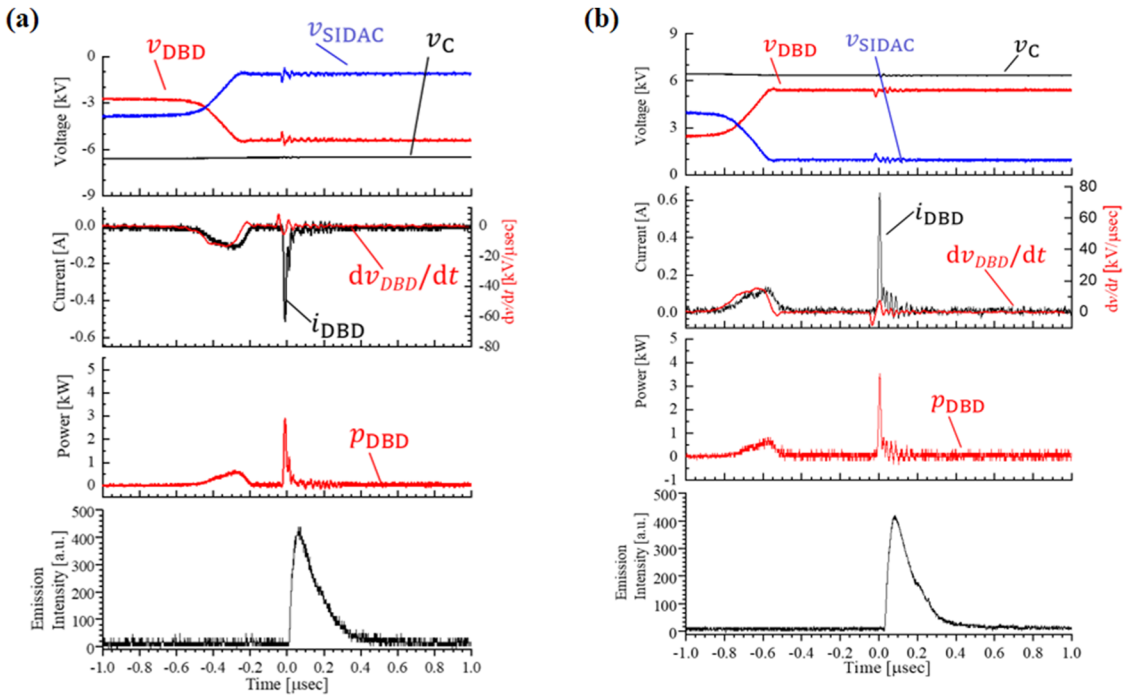

FIG. 6. Enlargement waveforms around typical discharges generated by unipolar pulses: (a) negative discharge and (b) positive discharge.

is kept constant to the absolute value of about 6.5 kV, and on the other side of the SIDAC connection, after each discharge, the voltage on the DBD reactor (v_{DBD}) is released through the voltage probe's internal resistance of 500 MΩ. After each discharge, the releasing charges on the DBD electrode make the voltage on the SIDAC connection increased back to the threshold value and prepared for the next discharges. On the other hand, in the case of DBD driven by bipolar pulses, the polarity of primary voltage imposing on one side of SIDAC connection (v_C) is alternated and reversed after each discharge. As a result, the conductive state of SIDAC or pulses imposing on the DBD reactor is mainly determined by the alternation in the polarity of primary voltage. Consequently, bipolar pulses or bipolar discharges are generated in each cycle of the applied primary AC voltage.

Figures 6 and 8 show enlargement waveforms around times when SIDACs are transiting to a conductive state, which means that pulses are generating and applying to the reactor. Figure 6 illustrates waveforms obtained with unipolar pulses in both uni-negative [Fig. 6(a)] and uni-positive [Fig. 6(b)] polarities. Figure 8 also illustrates enlargement waveforms obtained with bipolar pulses. From Figs. 6(a), 6(b), 8(a), and 8(b), it is visible that, for both unipolar DBD and bipolar DBD, in one voltage pulse duration, there is always the presence of two separate current peaks. The first current peak is the pure displacement current or capacitive current that appeared during the rising or falling slope of the high voltage pulse applied to the DBD reactor. This time, these currents are approximately proportional to the product of the high rise rate of the voltage applied to the DBD reactor (dv_{DBD}/dt) and the equivalent capacitance of the reactor (C_{DBD}) as an equation ($i = C_{DBD} \cdot \frac{dv_{DBD}}{dt}$). In all cases, the same reactor and the same rate of voltage change have been used; therefore, similar waveforms and similar peaks of about 0.2 A of displacement currents are observed. There is no discharge at this time; then, the photomultiplier tube (PMT) did not show any emission signals. The instantaneous power as a product of the voltage on the DBD electrode and the current during this time will be preserved in the reactor for the operation of the DBD.

The discharges only occur after the appearance of the first current peaks for a certain time. The discharges are detected by short surge currents lasting within tens of nanoseconds with a very high peak value accompanied with the light emission signal obtained by the (PMT) detector. These currents are pure conductive currents or referred to as discharge currents. Discharge current peaks are much higher than the peaks of displacement currents for all cases.

The lag between the time when the pulse applied and the discharge appeared is often called stochastic time lag.[26,30] This phenomenon has been explained in our previous study and is mainly caused by the prehistory effect of low operation frequency DBD operation in a glass reactor. The reason is mainly due to the influence of the property of glass on DBD characteristics. In this research, this lag is convenient for the investigation of the discharge mechanism since it splits between the displacement currents from discharge currents and, hence, essentially reduces the effect of parasite capacitance in the external circuit on discharge currents.

The big difference in discharge currents of DBDs generated by unipolar and bipolar pulses can be clearly observed in current waveforms enlarged around moments when the discharge occurred [Figs. 6(a), 6(b), 8(c), and 8(d)]. The peak of discharge currents in the case of bipolar DBD [Figs. 8(c) and 8(d)] is roughly three times

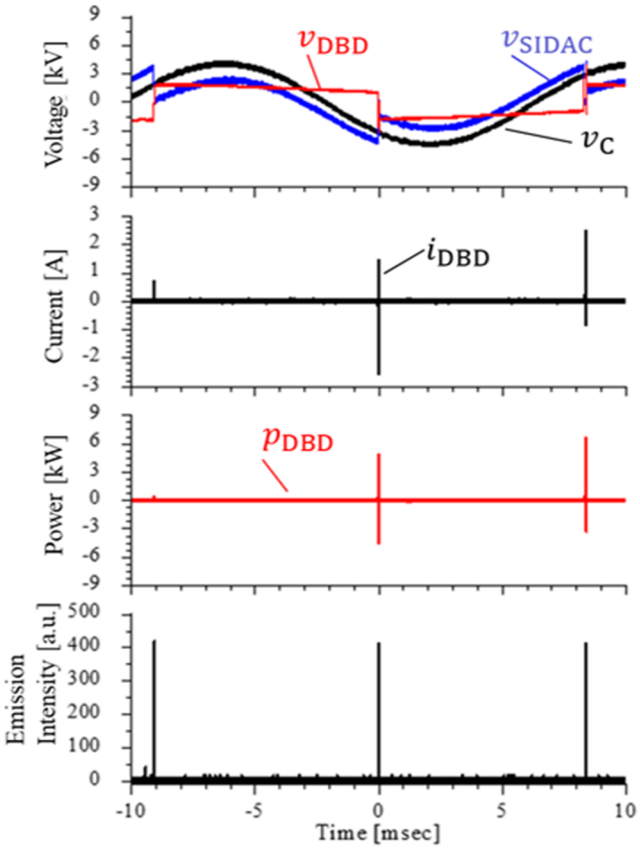

FIG. 7. Overall waveform of DBDs generated by bipolar pulses.

higher than those [Figs. 6(a) and 6(b)] of discharge currents in the case of unipolar DBDs. The very strong discharge in the case of DBD driven by bipolar pulses makes the magnitude of voltage on the DBD reactor after discharge occurring slightly reduced [Figs. 8(a) and 8(b)]. In contrast, in the case of DBD driven by unipolar pulses, the voltages on the DBD reactor are nearly unchanged when comparing the values at times right before and right after discharge occurring (Fig. 6). Energy consumption and the charge transfer over a discharge duration have also been estimated by integrating the power curves and current curves over the duration of discharge of several tens of nanoseconds. The charge exchange through the discharge in the case of bipolar DBD (about 23 nC, 3 nC) is higher than that in the case of unipolar DBD (about 17 nC, 4 nC), while the energy consumed by the discharge in the bipolar case (just about 0.055 mJ) is lower than the amount consumed by the discharge in the unipolar case (about 0.088 mJ).

The difference in the above electrical characteristics provides evidence of different mechanisms governing the two types of discharges. The fundamental mechanism behind the discrepancy in the electrical characteristic of the above two type DBDs is attributed to the build-up of charges on the dielectric surface and schematically illustrated in Figs. 9 and 10. Generally, when a high voltage pulse is applied to the reactor, a discharge occurs and is developed as a number of conductive channels illustrated in Figs. 9(a) and 10(a). Free charges are then forced to move under the orientation of the external electric field ($\vec{E}$) and accumulate on dielectric layers. The accumulation of charges on dielectric layers induces an electric field in the opposite direction to that of the external electric field ($\vec{E}$) and makes discharges terminated and prevents the ignition of discharge channels with the same polarity at the same locations. Hence, in the case of unipolar driven DBDs depicted sequentially in Figs. 9(a) and 9(b), unipolar consecutive DBDs cannot be sustained only by a direct current high voltage source with a fixed electric field. Therefore, after one discharge, the releasing of saturation points of the accumulated charged particles on the dielectric surface is critical for sustaining the unipolar DBDs. It can be seen from the experimental results shown in Fig. 5 that after a discharge taking place, the free charges on the electrodes of the DBD reactor are released through grounded 500 MΩ resistance of the HV voltage probe that is in parallel to the reactor. The above process is described in the schematic illustration shown in Figs. 9(b) and 9(c). The release of free charges is proposed as the cause of the redistribution of the structure of the induced charges in the dielectric layer, thus redistributing and diffusing the surface charges accumulated on the dielectric surface due to discharges from previous working cycles. As a result, the saturation points of the accumulated charged particles on the dielectric surface are partially erased [Fig. 9(c)]. Consequently, new discharges will be developed at new locations or points where the induced electric field is really weak [Fig. 9(d)]. However, energy stored by surface charges on the dielectric surface or in the discharge gap is also partially lost. In contrast, in the case of bipolar DBD generation, after a discharge taking place by applying a high voltage pulse in a half cycle of the primary power supply, the electric field induced by the accumulation of charged particles on the dielectric surface from the preceding discharge ($\vec{E}_{DBD}$) is in the same direction to that of the external field ($\vec{E}$) of the pulse applied to the reactor in the next half cycle of a primary power supply [Figs. 10(a) and 10(b)]. Therefore, the total net electric field in the discharge gap will be locally strongly enhanced along with points on the dielectric surface, where a large amount of charged particles are suspended [Fig. 10(c)]. Accordingly, the following discharge in the next half cycle with opposite polarity is then initiated under the total net electric field with abundant surface charges on dielectric layers and developed the conductive channels along with channels developed in preceding discharge time. The strong electric field leads to a strong discharge and a very high discharge current peak. In this case, the partial energy stored by surface charges on the dielectric surface from the preceding discharge has been employed for the following discharge, and that being the case of stronger discharge, higher charge is transferred but less energy is consumed by a discharge compared to those of the case of unipolar discharges.

Although the bipolar DBD plasma has advantages over the unipolar DBD plasma from the point of view of system efficiency, the unipolar DBD plasma can be ignited over the dielectric surface and sustain a large ratio of a surface over a volume of electric discharges at atmospheric pressure without limiting to narrow constricted locations as a bipolar DBD plasma since bipolar DBDs tend to be reignited at points where the previous discharge channels have already struck. This is an advantage of low-frequency DBD driven by a unipolar pulse with long falling time in specific applications such as

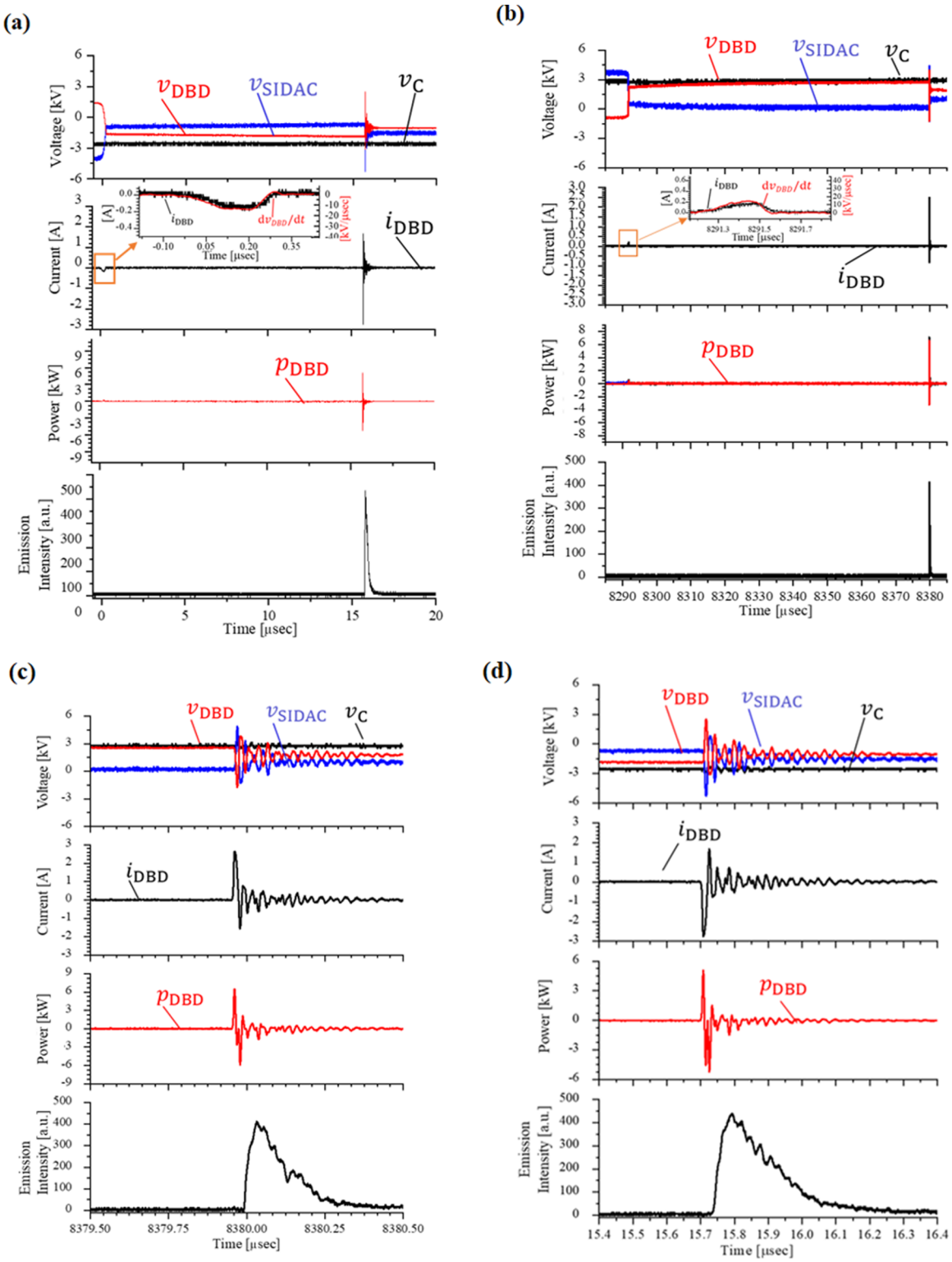

FIG. 8. Enlargement waveforms of DBDs generated by bipolar pulses: (a) waveform around time when a negative pulse is generated, (b) waveform around time when a positive pulse is generated, (c) enlargement waveform around a positive discharge, and (d) enlargement waveform around a negative discharge.

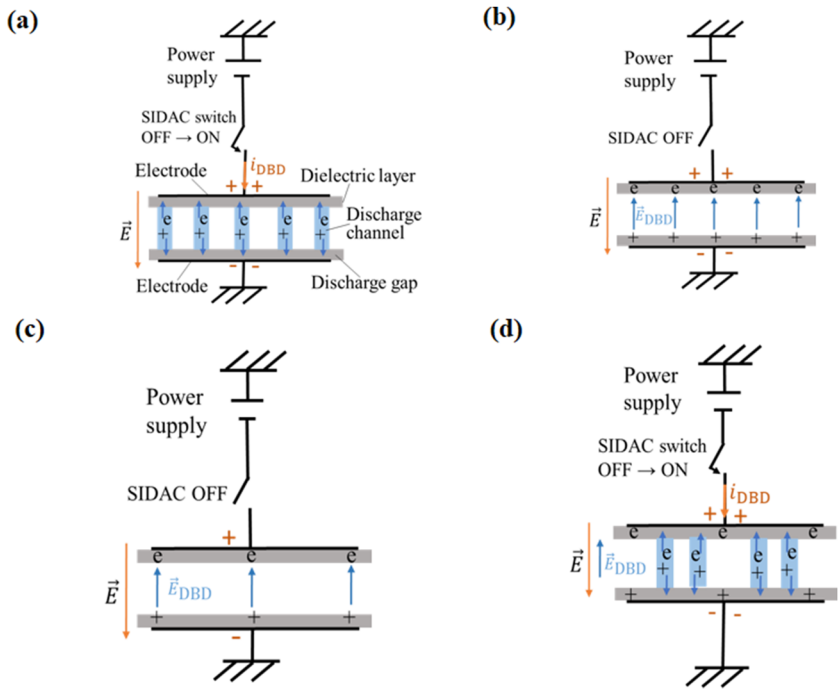

FIG. 9. Schematic of discharge development in the case of DBD driven by unipolar pulses: (a) schematic of discharge taking place, (b) discharge terminated by the induced electric field ($\vec{E}$ DBD), (c) charge accumulation on dielectric layers redistributed, and (d) next discharge developed at weakly charged areas.

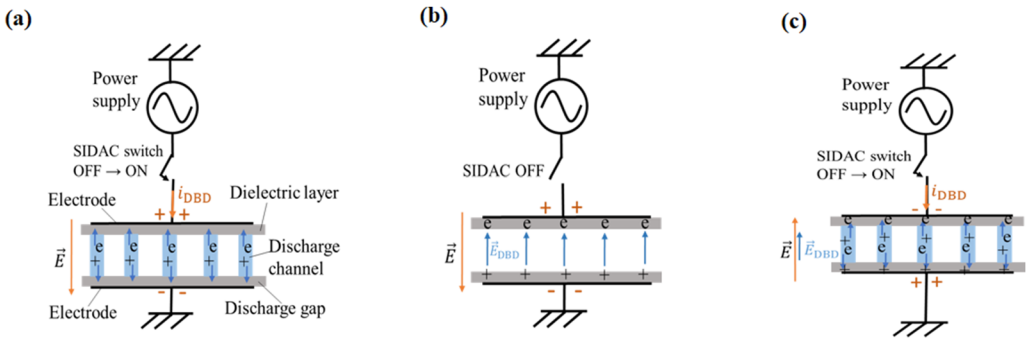

FIG. 10. Schematic of discharge development in the case of DBD driven by bipolar pulses: (a) schematic of discharge occurred by a positive pulse, (b) discharge terminated by the induced field ($\vec{E}$ DBD), and (c) next negative discharge ignited under a strong net field.

surface dielectric barrier discharge (SDBD) for flow actuators, electrohydrodynamic (EHD) control, which are beneficial from the negative saw-tooth waveform of the applied voltage and the diffusion of surface charges, or surface sterilization and surface processing.

V. CONCLUSION

This study has compared the mechanisms of development of the Dielectric Barrier Discharge (DBD) powered by low-frequency bipolar and unipolar pulses via measured electrical variables. The experimental results showed that discharge current peaks in the case of DBD driven by low-frequency repetitive unipolar pulses with long rise or fall time are about three times lower than those in the case of DBD driven by bipolar pulses. The big difference in the mechanism of the above two types of DBDs is attributed to the build-up and the diffusion of charges on the dielectric surface. In the case of the unipolar DBDs, the release of saturation points of the accumulated charged particles on the dielectric surface in the preceding discharge is critical for sustaining the unipolar DBDs. However, in the case of the bipolar DBDs, the excitation of the next discharge is beneficial from the memory effect due to charges accumulated on the surface of the dielectric layers in the previous pulse. In the view of energy efficiency, the bipolar DBD plasma has advantages over the unipolar DBD plasma. However, in specific applications such as surface dielectric barrier discharge (SDBD) for flow actuators or electrohydrodynamic (EHD) control, the mechanism driving the unipolar DBD plasmas may be more beneficial. This study has provided further understanding of the mechanism of the unipolar DBDs system,

where the use of low-frequency unipolar DBD with a long rise or fall time may be necessary for the low-cost operation or larger surface charge areas over a certain discharge volume.

ACKNOWLEDGMENTS

This research is funded by Funds for Science and Technology Development of the University of Danang under Project No. B2019-DN06-17.

DATA AVAILABILITY

The data that support the findings of this study are available from the corresponding author upon reasonable request.

REFERENCES

[1] U. Kogelschatz, Plasma Chem. Plasma Process. **23**, 1 (2003).
[2] H.-E. Wagner, R. Brandenburg, K. V. Kozlov, A. Sonnenfeld, P. Michel, and J. F. Behnke, Vacuum **71**, 417 (2003).
[3] Y. P. Raizer, *Gas Discharge Physics* (Springer, Berlin, 1991).
[4] J. R. Roth, *Industrial Plasma Engineering: Volume 2: Applications to Nonthermal Plasma Processing* (CRC Press, Boca Raton, FL, 2001).
[5] A. A. Abdelaziz, T. Ishijima, T. Seto, N. Osawa, H. Wedaa, and Y. Otani, Plasma Sources Sci. Technol. **25**, 035012 (2016).
[6] A. A. Abdelaziz, T. Ishijima, and T. Seto, Phys. Plasmas **25**, 043512 (2018).
[7] K. Kuroda, T. Ishijima, T. Kaga, K. Shiomomura, K. Ninomiya, and K. Takahashi, Chem. Lett. **44**, 1473 (2015).
[8] J. E. Foster, Phys. Plasmas **24**, 055501 (2017).
[9] K. Ninomiya, T. Ishijima, M. Imamura, T. Yamahara, H. Enomoto, K. Takahashi, Y. Tanaka, Y. Uesugi, and N. Shimizu, J. Phys. D: Appl. Phys. **46**(42), 425401 (2013).
[10] M. A. Jezeh, T. Tayebi, M. R. Khani, H. Niknejad, and B. Shokri, Plasma Processes Polym. **17**, 1900241 (2020).
[11] R. Brandenburg, Plasma Sources Sci. Technol. **26**, 053001 (2017).
[12] M. R. Pervez, T. Ishijima, A. Begum, Y. Tanaka, and Y. Uesugi, J. Phys. D: Appl. Phys. **52**, 065202 (2019).
[13] M. Kettlitz, H. Höft, T. Hoder, and K.-D. Brandenburg, Plasma Sources Sci. Technol. **22**, 025003 (2013).
[14] K. Takashima, Y. Zuzeek, W. R. Lempert, and I. V. Adamovich, Plasma Sources Sci. Technol. **20**, 055009 (2011).
[15] R. Dawson and J. Little, J. Appl. Phys. **113**, 103302 (2013).
[16] R. A. Dawson and J. Little, J. Appl. Phys. **115**, 043306 (2014).
[17] C. L. Enloe, T. E. McLaughlin, R. D. VanDyken, K. D. Kachner, E. J. Jumper, T. C. Corke, M. Post, and O. Haddad, AIAA J. **42**(3), 595 (2004).
[18] G. Tathiri, E. Esmaeilzadeh, S. M. Mirsajedi, and H. M. Moghaddam, J. Appl. Fluid Mech. **7**(3), 525–534 (2014).
[19] Y. Akishev, G. Aponin, A. Balakirev, M. Grushin, V. Karalnik, A. Petryakov, and N. Trushkin, J. Phys. D: Appl. Phys. **46**, 464014 (2013).
[20] N. Benard and E. Moreau, Exp. Fluids **55**, 1846 (2014).
[21] F. O. Thomas, T. C. Corke, M. Iqbal, A. Kozlov, and D. Schatzman, AIAA J. **47**, 2169 (2009).
[22] R. V. Dyken, T. McLaughlin, and C. Enloe, AIAA Paper 2004-0846, 2004.
[23] L. Zhang, D. Yang, W. Wang, Z. Liu, S. Wang, P. Jiang, and S. Zhang, J. Appl. Phys. **116**, 113301 (2014).
[24] S. Liu and M. Neiger, J. Phys. D: Appl. Phys. **34**, 1632 (2001).
[25] X. Lu and M. Laroussi, J. Appl. Phys. **100**, 063302 (2006).
[26] H. T. Truong, Y. Uesugi, Y. Tanaka, and T. Ishijima, Jpn. J. Appl. Phys., Part 1 **58**, 111001 (2019).
[27] M. A. Malik, K. H. Schoenbach, T. M. Abdel-Fattah, R. Heller, and C. Jiang, Plasma Chem. Plasma Process. **37**, 59 (2017).
[28] H. T. Truong, M. Hayashi, Y. Uesugi, Y. Tanaka, and T. Ishijima, Rev. Sci. Instrum. **88**, 065105 (2017).
[29] Y. Sumiishi, Y. Uesugi, Y. Tanaka, and T. Ishijima, J. Phys.: Conf. Ser. **441**, 012018 (2013).
[30] P. Fu, Z. Zhao, X. Li, X. Cui, and Z. Yang, Phys. Plasmas **25**, 093518 (2018).